https://doi.org/10.20965/jaciii.2009.p0289

Paper:

A Genetic-Algorithm-Based Temporal Subtraction for Chest Radiographs

Takeshi Inaba*, Lifeng He*, Kenji Suzuki, Kazuhito Murakami*, and Yuyan Chao*****

*Graduate School of Information Science and Technology Aichi Prefectural University, Nagakute-cho, Aichi 480-1198, Japan
E-mail: {im081004, helifeng, murakami}@ist.aichi-pu.ac.jp
**Department of Radiology, Division of Biological Sciences, The University of Chicago, 5841 South Maryland Avenue, Chicago, IL 60637, USA
E-mail: suzuki@uchicago.edu
***Graduate School of Environmental Management, Nagoya Sangyo University, Owariasahi-city, Aichi 488-8711, Japan
[Received November 25, 2008; accepted February 25, 2009]

To assess pathological chest change, radiologists compare the same patient's chest radiographs taken at different times. Supporting radiologists' diagnostics, temporal-subtraction images constructed from the previous and current radiographs have enhanced the visualization of pathological change. This paper presents a genetic-algorithm-based temporal subtraction for chest radiographs. First, we extract ribs from previous and current images and use them for global matching of the two images. Then, we divide the lung area in the current image into many subareas. For individual subarea, we use the genetic algorithm for local matching to find its corresponding area in the previous image efficiently. Results demonstrated that pathological change were accurately enhanced in temporal-subtraction images without major misregistration artifacts, accurately visualizing of pathological change and proving useful in improving radiologists, diagnostic performance.

Keywords: temporal-subtraction image, computer aided diagnosis (CAD), genetic algorithm (GA), medical imaging, image registration

1. Introduction

Since 1981, the number of deaths due to cancer have held first places as a cause of death in Japan. The number of deaths due to lung cancer alone occupied first place for men as well as men and women combined in 2005 [1].

To reduce the deaths due to lung cancer, early detection of cancer is the most important. Chest radiography has been used for detection of lung cancer and is the most frequently used imaging modality for this diagnostic purpose.

To assess pathological change (generation and progress) in chest radiographs, radiologists often compare the previous and current chest radiographs obtained from the same patient at different times. To support radiologists' diagnostic work, temporal-subtraction images constructed by use of the previous and current radiographs have been developed for the enhanced visualization of pathological change. Temporal-subtraction images can reduce radiologists' mass screening load and minimizes oversights of pathological change overlapping with ribs and clavicles.

Because the previous and current radiographs are taken at different times have different photographic conditions, e.g., the patient's position and x-ray conditions, making accurate image registration technically challenging. Artifacts due to temporally subtracted images lead to misregistration that may lead to misdiagnosis. This makes improving registration accuracy crucial.

Image registration has been proposed using global matching [2] for constructing temporal-subtraction images, in the lung area followed by local matching [3] to correct misregistrations in local areas. Automated evaluation method [4] has been developed registration accuracy in temporal-subtraction images.

This paper presents the genetic-algorithm-based temporal subtraction (GABTS) for chest radiographs. First, we extract ribs from previous and current radiographs, for global matching the two images. Then, we divide the lung area in the current image into many local subareas. For individual local subarea, we use a genetic algorithm for local matching to efficiently find its corresponding area in the previous image. In local matching, calculating the shift vector as previously proposed in researchers method, we take into account rotation and magnification for individual local subarea to improve accuracy.

This paper is organized as follows: section 2 introduces rib-image-based global matching method, section 3 introduces genetic-algorithm-based local matching. Section 4 explains how to reconstruct the previous radiograph. Section 5, shows and discuss experimental results, and section 6 presents conclusion.

2. Global Matching by Use of Rib-Edge Images

We used original previous and current radiographs (**Fig. 1 (a)** and **(b)**).

In this paper, we often discuss pathological change and misregistration artifacts. The pathological changes

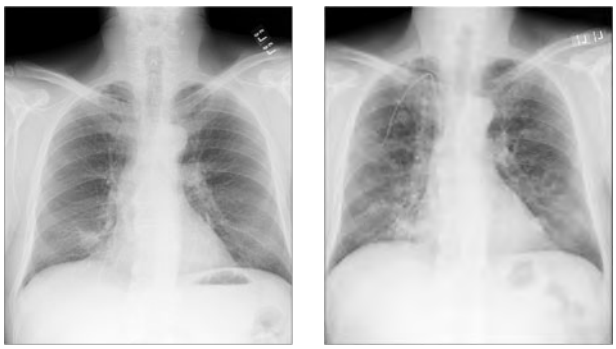

(a) (b)

Fig. 1. Original radiographs used in temporal subtraction: (a) previous radiograph and (b) current radiograph (the same patient).

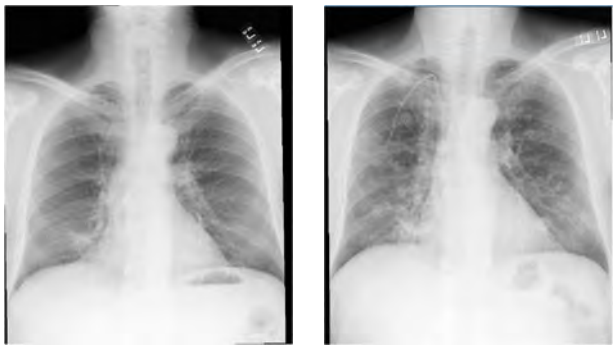

(a) (b)

Fig. 2. Images after rotation and horizontal shift: (a) previous image and (b) current image.

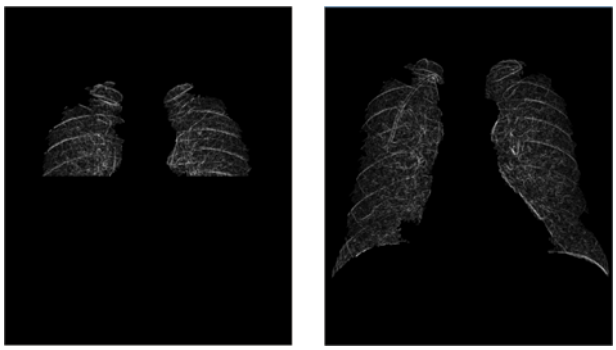

(a) (b)

Fig. 3. Rib-edge extracted from (a) previous image and (b) current image.

(a) (b)

Fig. 4. Images after global matching (rib-edge matching): (a) previous image and (b) current image.

in constructed temporal subtraction images are bright, caused by pathological changes occurring in the same place in the current but not the previous image. Misregistration artifacts are either very dark or very bright areas in the constructed temporal subtraction image caused by misregistration, i.e., no pathological change actually exists in the current image.

Global matching of previous and current radiographs involves rotation, horizontal shifting, and rib-edge matching.

Similar to the previous method proposed in Ref. [2], we first find the lung midline in radiograph, rotating the image until the midline is vertical to the horizontal axis on the image plane. Then, we shift the image horizontally until the midline becomes the image center line (**Fig. 2**).

Next, we extract rib edges in the lung area using of the Sobel operator [5] (**Fig. 3**), then, move the previous rib-edge image up or down within a certain range to minimize the average absolute error of all image pixels, i.e., after global matching (**Fig. 4**).

Conventional global matching [2] cross-correlation pixels of the two images, extracting the upper ribcage from the previous image and using the entire ribcage image from the current image.

we used rib-edge images for global matching. Because the same patient's upper ribs would not change greatly in size and shape, using rib-edge images in global matching potentially produces more accurate results than in original images used previously (**Fig. 5 (a)**, **(b)**, and **(c)**).

Visualization of pathological changes is improved in both subtraction images generated using previous global matching and our method, compared to the subtraction image generated by use of the original radiographs directly (*direct subtraction*) (**Fig. 5 (c)**). As marked areas show, the artifact in the subtraction image generated using the previous method is more obvious than that in our subtraction image, showing how our global matching improves registration accuracy.

The histogram of pixel values in the lung area in direct subtraction (**Fig. 5 (c)**), and that in GABTS (**Fig. 5 (b)** and **Fig. 6**).

Figure 6 indicates that contrast in GABTS is lower than that of direct subtraction images. The quality of the GABTS image (**Fig. 5 (b)**) is much better than that generated by direct subtraction (**Fig. 5 (c)**).

3. Genetic-Algorithm-Based Local Matching

Genetic-algorithm-based local matching (GABLM) consists of two processes: (1) construction of template subareas in the ribcage area in the current image, and (2) searching for an area corresponding to individual template subareas in the previous image using of the genetic algorithm.

For (1), similar to the previous method proposed in

(a) (b) (c)

Fig. 5. Temporal-subtraction images generated by previous and current radiographs after global matching in (a) previous method, (b) our method, (c) the original radiographs without global matching.

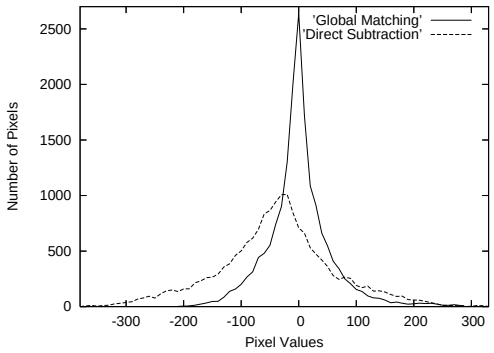

Fig. 6. Comparison of histograms of pixel values in lung in temporal-subtraction images generated by direct subtraction and our method.

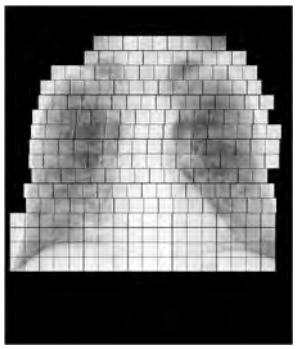

Fig. 7. Example of constructed template subareas in ribcage in current image.

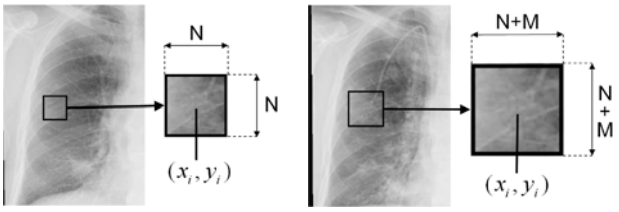

(a) (b)

Fig. 8. Example of the subareas: (a) template subarea in current image and (b) corresponding search subarea in the previous image.

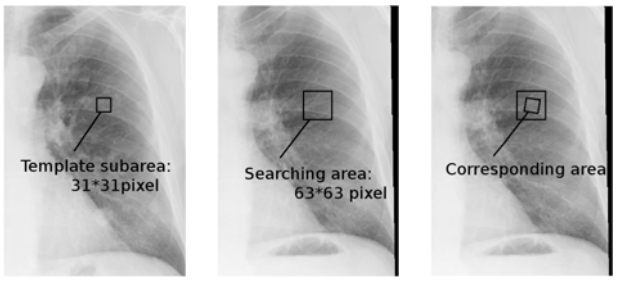

(a) (b) (c)

Fig. 9. Example of local matching: (a) template subarea in current image, (b) corresponding search subarea in previous image, (c) corresponding area in previous image.

Ref. [2], we calculate the ribcage from the lung mask in the current image, then divide the ribcage area using raster scanning into $N \times N$-size subareas, where N is an odd number (**Fig. 7**). For each template subarea in the current image, we must find its corresponding area in the previous image. Because global matching was made in advance, we limit local matching to that completed in the $(N+M) \times (N+M)$-size subarea, where M is an optional number with the same template subarea center coordinate in the previous image, i.e., a *search subarea* (**Fig. 8**).

Considering the characteristics of changes in radiographs taken at different times.

We search for an area corresponding to a template subarea in the current radiograph in the search subarea of the previous radiograph as follows: (1) vertical shift, (2) horizontal shift, (3) rotation, and (4) magnification. These operations generate a huge number of candidate subareas. Consequently, it is difficult to check all subareas one by one. The genetic algorithm finds an optimal/quasi-optimal solution from a huge number of candidate solutions, so we use it for local matching (**Fig. 9**).

We define a genetic algorithm set for local matching, which includes a genotype, the fitness function, and parameters:

Our genotype has 23 bits: 6 bits each for the *x* axis and *y* axis of the center of the corresponding area in the search subarea of the previous image, 5 bits for the angle of rotation, and 6 bits for the magnification factor. Because local matching is executed after global matching, rotation range is limited to $[-15, 15]$ and the magnification range to $[0.8, 1.2]$.

The fitness function for evaluating an individual is de-

fined as:

$$sum = \sum_{i=1}^{N\times N} \begin{cases} if\,(0\leq i<N+M)\,and\,(0\leq j<N+M) \\ \qquad |f(x_i,y_j)-g(x_i,y_j)| \\ else \qquad max-min \end{cases} \quad . \quad (1)$$
$$fitness = 1 - sum/(N^2 \times (max-min))$$

where $f(x_i,y_i)$ and $g(x_i,y_i)$ are the pixel values at (x_i,y_i) of the template subarea in the current image and the search subarea in the previous image, $N \times N$ is the number of pixels in the template subarea, $(N+M)$ is the $(N+M)\times(N+M)$-size of the search subarea, *max* and *min* are maximum and minimum pixel values in the template subarea and the search subarea, *sum* is a total of the absolute pixel value difference of all $f(x_i,y_i)$ and $g(x_i,y_i)$, and *fitness* is the value of the fitness ranges from 0 to 1. The larger an individual's fitness, the better the individual.

In our genetic algorithm: the number of individuals is 100, that of maximum generations is 100, that of crossover points is two, the crossover rate is 80%, the mutation rate is 1%, the end condition is set so that the fitness exceeds 0.99, or the generation reaches the limit.

4. Previous-Radiograph Reconstruction

For each template subarea with center (i,j) in the current image, in the previous image, we construct a subarea of the same size (i.e., $N \times N$) and the same center (i.e.,(i,j)) using the corresponding subarea found by GABLM for the reconstructed previous image (**Fig. 10**). $\mathscr{S}(T,a,b,r)$ denotes a subarea with size $T \times T$, center (a,b), and inclination angle r with the horizontal axis.

Figure 10 (a) shows a template subarea $\mathscr{S}_1(N,i,j,0)$ in the current image, **Fig. 10 (b)** the search subarea $\mathscr{S}_2(N+K,i,j,0)$ in the previous image, **Fig. 10 (c)** the corresponding subarea $\mathscr{S}_3(N\times\alpha, i+m, j+n, \beta)$ found by GABLM in the search subarea, where α is expanding magnification and β the rotating angle decided by the genetic algorithm. **Fig. 10 (d)** demonstrates the operations for constructing the subarea for the reconstructed previous image using subarea $\mathscr{S}_3(N\times\alpha, i+m, j+n, \beta)$, i.e., expanding subarea $\mathscr{S}_3(N\times\alpha, i+m, j+n, \beta)$ by expanding magnification $1/\alpha$, moving it $-m$ horizontally and $-n$ vertically, and rotating it $-\beta$ clockwise. Lastly, **Fig. 10 (e)** shows the constructed subarea $\mathscr{S}_4(N,i,j,0)$ for the reconstructed previous image.

For each template subarea $\mathscr{S}_c(N,i,j,0)$ in the current image, we construct corresponding subarea $\mathscr{S}'(N,i,j,0)$ for the reconstructed previous image. By replacing each subarea $\mathscr{S}_p(N,i,j,0)$ in the previous image with subarea $\mathscr{S}'(N,i,j,0)$, we obtain the reconstructed previous image.

Some reconstructed previous images will be given later in the next section.

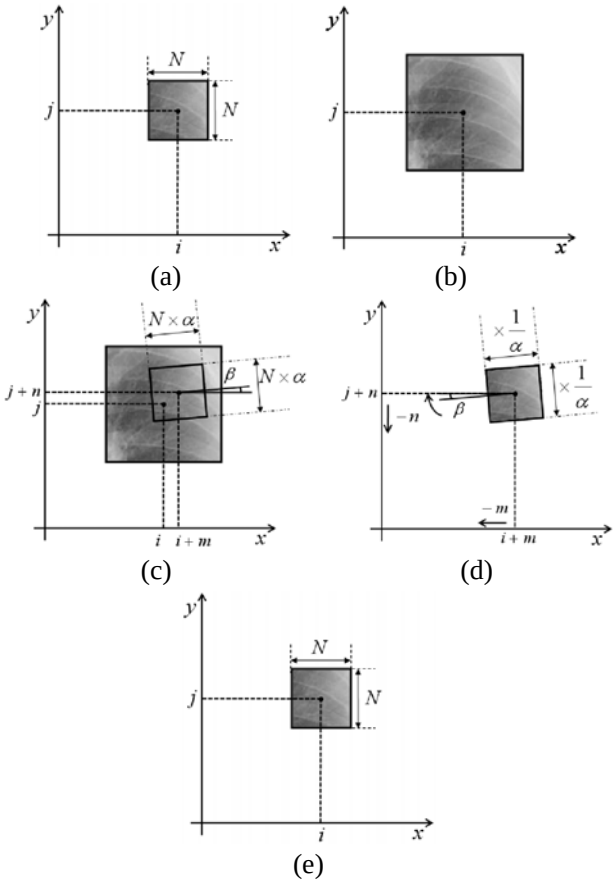

Fig. 10. Example for reconstructing subarea in previous radiograph: (a) template subarea in current image; (b) search subarea in previous image; (c) corresponding subarea in searching area; (d) operations for constructing subarea for reconstructed previous image; (e) constructed subarea for reconstructed previous image.

5. Results and Discussion

5.1. Temporal-Subtraction Images Constructed Using of Different Template Subarea Sizes

We construct the temporal-subtraction image using the reconstructed previous image and the current image after global matching (**Fig. 2 (b)**).

We use $I_p(N,N+M)$ and $I(N,N+M)$ to denote the reconstructed previous image and the temporal-subtraction image constructed by using $N\times N$-size template subareas and $(N+M)\times(N+M)$-size search subareas. $I_p(21,31)$, $I_p(21,42)$ and $I_p(41,62)$ are shown in **Fig. 11 (a)**, **(b)** and **(c)**. $I(21,31)$, $I(21,42)$ and $I(41,62)$ are also shown in **Fig. 12 (a)**, **(b)** and **(c)**.

Comparing $I(21,31)$ (**Fig. 12 (a)**) and $I(41,62)$ (**Fig. 12 (c)**) shows that misregistration artifacts and discontinuous areas in $I(21,31)$ are much smaller than that in $I(41,62)$, especially for the area marked by an oval. This is because, with a smaller template subarea, misregistration can be corrected more in detail, and the discontinuous areas between neighboring corresponding areas are suppressed. Smaller template subareas should thus be used for local matching.

(a) (b) (c)

Fig. 11. Reconstructed previous images: (a) $I_p(21,31)$, (b) $I_p(21,42)$, (c) $I_p(41,62)$.

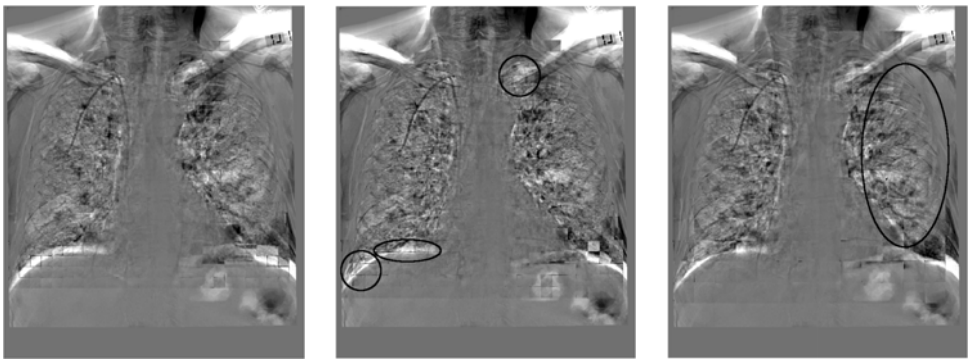

(a) (b) (c)

Fig. 12. Constructed temporal-subtraction images: (a) $I(21,31)$, (b) $I(21,42)$, (c) $I(41,62)$.

Because a better corresponding area can be found in a larger search subarea, a larger search subarea should be used. We confirmed that the misregistration artifacts in the marked areas in $I(21,42)$ (**Fig. 12 (b)**) are smaller than that in $I(21,31)$.

Enhanced pathological changes in $I(21,31)$ are more obvious than in $I(21,42)$.

We use 21×21 template subareas and 31×31 search subareas, so $I(21,31)$ (**Fig. 12 (a)**) is the temporal-subtraction image we constructed.

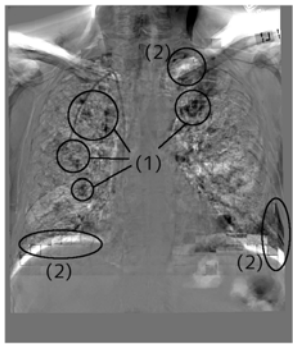

Fig. 13. Temporal-subtraction image with noteworthy points.

5.2. Evaluation

We evaluated temporal-subtraction image quality two ways:

First we used a physical measurement with the histogram of pixel values in the lung of a subtraction image. Because misregistration areas contain many very dark or very bright pixels, a high-quality subtraction image usually has low contrast, i.e., the width of its histogram is narrow. Inversely, a poor quality subtraction image often has high contrast, i.e., the width of its histogram is wide.

Second, we used subjective observation of the subtraction image, checking whether pathological change are enhanced and the amount of misregistration artifacts in the image. We evaluated temporal-subtraction images by subjective observation (**Fig. 13**) where pathological change are marked by (1) and misregistration artifacts by (2). Note that only a few misregistration artifacts and pathological change are enhanced accurately. Compared to the temporal-subtraction image constructed after global matching (**Fig. 5 (b)**), obscure areas decreased notably in the subtraction image constructed after local matching. Artifacts in ribcage edges, the upper lung, the lower lung area, and the right rib edge also decreased in number. We then evaluated the temporal-subtraction image constructed using the histogram of pixel values (**Figs. 14** and **6**) The temporal-subtraction image constructed after local matching has the highest, steepest peak and the narrowest width, i.e., contrast of the temporal-subtraction image constructed after local matching is further weakened. For the same reasons mentioned above, we know that the quality of the subtraction image is further improved after local matching.

Therefore, local matching effectively corrects local and complex misregistration and distortion in the ribcage area

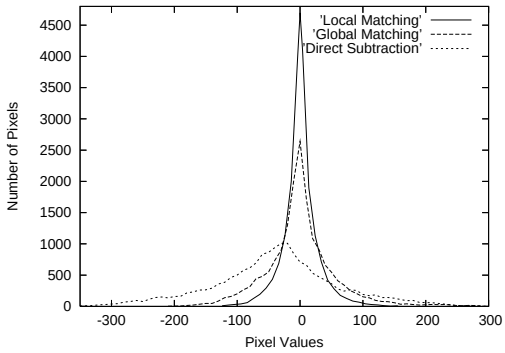

Fig. 14. Histograms of pixel values (**Fig. 5 (b)**, **Fig. 5 (c)**, and **Fig. 13**).

between previous and current radiographs.

5.3. Projected Work

We face two tasks: (1) improving the quality of temporal-subtraction images and (2) improving evaluation.

A larger search subarea makes it possible to find more suitable corresponding areas (**Fig. 12 (b)**). Using our current method may, however, decrease misregistration artifacts while limiting the enhancement of pathological changes.

Because both areas of pathological change and rib areas have high pixel values, misregistration may easily arise for a template subarea in pathological change areas if its corresponding search subarea contains rib areas. This problem becomes more obvious when a larger search subarea is used (**Fig. 15**). **Fig. 15 (a)** shows the location of a template subarea, which is in a pathological change area, in the current image, and **Fig. 15 (b)**, the search subarea, which contains some rib areas, in the previous image, **Fig. 15 (c)**, the enlarged template subarea and the search subarea, where the slashing area in **Fig. 15 (d)** indicates the rib area in the search subarea, **Fig. 15 (e)**, a mismatching result, and **Fig. 15 (f)**, a good matching.

As a resolution, after obtaining a suitable solution for a template subarea, we compare the results of vertical and horizontal shift, rotation, and magnification, with those in corresponding subareas around the solution. If the four operations are against the others on the around subareas, we abandon the solution, and use the solution calculated by averaging the solutions of the around subareas.

We also find a more suitable corresponding area by calculating the fitness value using another method, e.g., based on cross-correlation.

We directly replace search subareas processed by suitable solutions in local matching. To prevent discontinuous areas, we should interpolate pixel values of surrounding subareas.

To evaluate the temporal-subtraction image, we used the histogram of pixel values in the lung area as an objective measure, but more objective evaluation is needed to make evaluation more accurate.

Researchers have developed a technique for suppressing ribs in chest radiographs [6]. We will incorporate this rib-suppression technique into our temporal subtraction technique to further reduce rib artifacts.

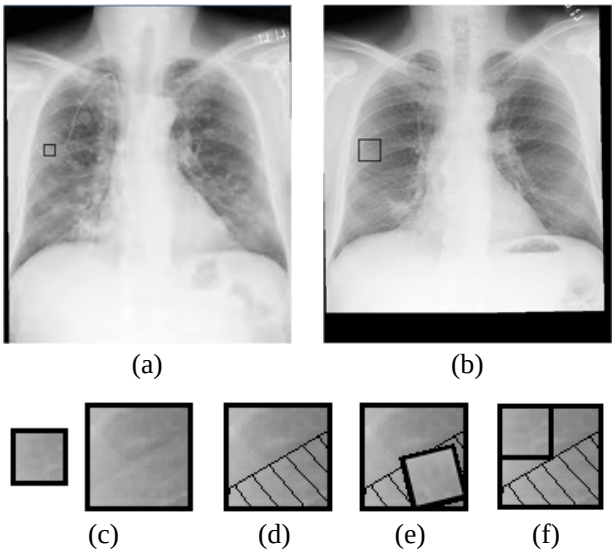

Fig. 15. Example explaining mismatching: (a) location of template subarea with pathological change in the current image, (b) corresponding searching area in previous image, (c) enlarged template subarea (left) and searching area (right), (d) rib area (slashed area) in search subarea, (e) poor matching result, (f) good matching.

5.4. Comparison with Other Optimization Methods

Beside the genetic algorithm, the steepest decent method (SDM) [7] and further davidon fletcher powell (DFP) [8] can be used to select resolution, but they the two methods only guarantee convergence of local minimum, and the cost function should be differentiated. In comparison, our genetic algorithm is convergent high possibility to obtain an approximate value of the global minimum, and therefore is better for our purpose.

6. Conclusions

Gnetic-algorithm-based temporal subtraction we propose for chest radiographs corrects misregistration caused by patient positioning among previous and current images. Experimental results demonstrated that pathological changes in temporal-subtraction images were enhanced accurately with few misregistration artifacts. We plan to improve the system and test it more extensively.

Acknowledgements

This work was supported in part by the Toyoaki Scholarship Foundation of Japan.

References:

[1] National Cancer Center: Cancer information service, http://ganjoho.ncc.go.jp/public/index.html

[2] T. Ishida, K. Ashizawa, R.M. Engelmann, S. Katsuragawa, H. MacMahon, and K. Doi, "Application of temporal subtraction for

detection of interval changes in chest Radiographs: Improvement of subtraction image using automated initial image matching," Journal of Dig Imag, Vol.12, No.2, pp. 77-86, 1999.

[3] T. Ishida, S. Katsuragawa, K. Nakamura, H. MacMahon, and K. Doi, "Iterative image warping technique for temporal subtraction of sequential chest radiographs to detect interval change," Med Phys, Vol.26, No.7, pp. 1320-1329, 1999.

[4] S. G. Armato III, D. J. Doshi, R. Engelmann, C. L. Croteau, and H. MacMahon, "Temporal subtraction in chest radiography: Automated assessment of registration accuracy," Med Phys, Vol.33, No.5, pp. 1239-1249, 2006.

[5] I. Seiki, H. Masaki, M. Koji, Y. Nobuyuki, N. Eisuke, and O. Masato, "C gengo de manabu jissen gazo shori -Windows, Machintosh, X-Window taiou-," Ohmsha, 1999 (in Japanese).

[6] K. Suzuki, H. Abe, H. MacMahon, and K. Doi, "Image-processing technique for suppressing ribs in chest radiographs by means of massive training artificial neural network (MTANN)," IEEE Trans Med Imaging, Vol.25, No.4, pp. 406-416, 2006.

[7] H. Masahumi, "Neuro/Fuzzy/Genetic Algorithm," Sangyo-Tosho, 2003 (in Japanese).

[8] R. Fletcher and M. J. D. Powell, "A Rapidly Convergent Descent Method for Minimization," Computer Journal, Vol.6, pp. 163-168, 1963.

Name:
Takeshi Inaba

Affiliation:
Graduate School of Information Science and Technology, Aichi Prefectural University

Address:
Nagakute-cho, Aichi 480-1198, Japan

Brief Biographical History:
2008- Graduate Student, Aichi Prefectural University, Japan

Main Works:
• "A Genetic-Algorithm-Based Method for Temporal Subtraction in Chest Radiography," Joint 4th International Conference on Soft Computing and Intelligent Systems and 9th International Symposium on advanced Intelligent Systems, pp. 1619-1624, Nagoya, Sep., 2008.

Name:
Lifeng He

Affiliation:
Graduate School of Information Science and Technology, Aichi Prefectural University

Address:
Nagakute-cho, Aichi 480-1198, Japan

Brief Biographical History:
1997 Received Ph.D. degrees in AI and computer science from Nagoya Institute of Technology, Japan
1999- Associate Professor, Aichi Prefectural University, Japan
2006-2007 Research Associate, the University of Chicago, USA

Main Works:
• "Fast Connected-Component Labeling," Pattern Recognition, Accepted (DOI: 10.1016/j.patcog.2008.10.013)
• "A Run-based Two-Scan Labeling Algorithm," IEEE Transactions on Image Processing, Vol.17, No. 5, pp. 749-756, 2008.

Membership in Academic Societies:
• The Associate for Automated Reasoning (AAR)

Name:
Kenji Suzuki

Affiliation:
Department of Radiology and Graduate Program in Medical Physics, Division of the Biological Sciences, The University of Chicago

Address:
5841 South Maryland Avenue, Chicago, IL 60637, USA

Brief Biographical History:
1993- Research and Development Center, Hitachi Medical Corporation
1997- Department of Applied Information Science and Technology, Faculty of Information Science and Technology, Aichi Prefectural University
2001- Department of Radiology, Division of the Biological Sciences, The University of Chicago

Main Works:
• "Neural edge enhancer for supervised edge enhancement from noisy images," IEEE Transactions on Pattern Analysis and Machine Intelligence, Vol.25, pp. 1582-1596, Dec. 2003.
• "Computer-aided diagnostic scheme for distinction between benign and malignant nodules in thoracic low-dose CT by use of massive training artificial neural network," IEEE Transactions on Medical Imaging, Vol.24, pp. 1138-1150, Sept. 2005.
• "Image-processing technique for suppressing ribs in chest radiographs by means of massive training artificial neural network (MTANN)," IEEE Transactions on Medical Imaging, Vol.25, pp. 406-416, April 2006.

Membership in Academic Societies:
• Senior Member, Institute of Electrical and Electronics Engineers (IEEE)
• American Association of Physicists in Medicine (AAPM)
• Institute of Electronics, Information and Communication Engineers (IEICE)

Name:
Kazuhito Murakami

Affiliation:
Graduate School of Information Science and Technology, Aichi Prefectural University

Address:
Nagakute-cho, Aichi 480-1198, Japan

Brief Biographical History:
1984 B.S. degree in Physics from Nagoya University
2002 Ph.D. degree in Engineering from Nagoya University
1991-1998 Senior Assistant Professor, Cukyo University
2007- Professor, Aichi Prefectural University, Japan

Main Works:
• "High Speed Line Detection Method Using Hough Transform in Local Area," The transactions of the Institute of Electronics, Information and Communication Engineers (IEICE), Vol.J83-D-II(3), pp. 918-926, 2000.

Membership in Academic Societies:
• The Institute of Electronics, Information and Communication Engineers (IEICE)
• The Information Processing Society of Japan (IPSJ)
• Japanese Society for Artificial Intelligence (JSAI)

Name:
Yuyan Chao

Affiliation:
Graduate School of Environmental Management, Nagoya Sangyo University

Address:
Owariasahi-city, Aichi 488-8711A, Japan

Brief Biographical History:
2000 The Ph.D degrees from Nagoya University, Japan
2000-2002 Special Foreign Researcher of Japan Society for the Promotion of Science, Nagoya Institute of Technology
2005 Assistant Professor, Nagoya Sangyo University, Japan
2008- Associate Professor, Nagoya Sangyo University, Japan

Main Works:
• "R-UNSEARCHMO: A Refinement on UNSEARCHMO PRICAI2002," Trends in Artificial Intelligence, Vol.2417, pp. 29-3, 2002

Membership in Academic Societies:
• Japanese Society for Artificial Intelligence (JSAI)